

Slow magnetic relaxation in a cobalt magnetic chain

Chen-I Yang,^a Po-Hsiang Chuang,^{a,b} Kuang-Lieh Lu^{a,*}

^aInstitute of Chemistry, Academia Sinica, Taipei 115, Taiwan; ^bGraduate Institute of Engineering, National Taiwan University of Science and Technology, Taipei 106, Taiwan

	Index	Page
	Experimental section	S2
Table 1S.	Crystallographic data for complex 1 .	S4
Figure 1S.	2D layer structure of 1 connected by H bonding.	S5
Figure 2S.	Plot of χ_M^{-1} (\circ) vs. temperature for a microcrystalline sample of complex 1 . The solid line represents the best fit χ_M^{-1} above 50 K with a Curie–Weiss law.	S6
Figure 3S.	ZFC/FC magnetization for 1 at an applied field of 50 G.	S7
Figure 4S.	Plots of in-phase (χ_M') of ac susceptibility vs. frequency in a 3.5 G ac field oscillating at the indicate temperatures for complex 1 .	S8
Figure 5S.	Plots of in-phase ($\chi_M'T$) (Top) and out-off-phase (χ_M'') (Bottom) of ac susceptibility vs. T in a 3.5 G ac field oscillating at the indicate frequencies for complex 1 .	S9
Figure 6S.	Plot of $\ln(\chi_M T)$ vs. T^{-1} for 1 . Solid line represents the fit of $\chi T = C_{\text{eff}} \exp(\Delta_{\text{E}}/k_B T)$ between 8 and 14 K.	S10
Figure 7S.	Plot of C_p vs. T for a pellet piece polycrystalline of 1 measured on grounded crystals under zero applied field.	S11

Synthesis:

A solution of 2,3-dihydroxyquinoxaline (164.3 mg, 1.0 mmol) and $\text{Co}(\text{OAc})_2 \cdot 4\text{H}_2\text{O}$ (251.8 mg, 0.99 mmol) in 10 mL of THF and 0.25 mL of NEt_3 was sealed in a Teflon-lined stainless steel vessel (23 mL). The mixture was heated according to the following temperature program: increasing the temperature to 140 °C at 18.3 °C/h, holding at 140 °C for 72 h, and then cooling to 30 °C at a rate of 2.3 °C/h. The deep purple block crystals suitable for single-crystal X-ray diffraction analysis were obtained. The crystals were rinsed a few times with DMF and ether, and dried in air. Yield: 67.8%. Anal. calcd for $\text{C}_{10}\text{H}_8\text{CoN}_2\text{O}_4$: C, 43.03; H, 2.89; N, 10.04. Found: C, 42.63; H, 2.62; N, 9.73.

X-ray Crystallography. Diffraction measurements for complex **1** were carried out using a Bruker APEXII CCD diffractometer with graphite-monochromated Mo K_α radiation ($\lambda = 0.7107 \text{ \AA}$). Data collation parameters of **1** are listed in Table S1. Structure was solved by direct methods and refined using the SHELXL-97¹ program by full-matrix least-squares on F^2 values. All non-hydrogen atoms were refined anisotropically, whereas the hydrogen atoms were placed in ideal, calculated positions, with isotropic thermal parameters riding on their respective carbon atoms.

Magnetic measurement. Variable temperature dc magnetic susceptibility measurements were collected on microcrystalline samples, restrained in eicosane to prevent torquing, on a Quantum Design MPMS SQUID-VSM magnetometer equipped with a 7.0 Tesla magnet and operating in the range of 1.8–300.0 K. AC magnetic susceptibility were performed on aligid on a Quantum Design MMPS magnetometer. Diamagnetic corrections were estimated from

Pascal's constants² and subtracted from the experimental susceptibility data to obtain the molar paramagnetic susceptibility of the compounds. Measurements of the heat capacity for a polycrystalline sample (pellet piece) of complex **1** between $T = 1.8$ K and $T = 20$ K were made by a Quantum Design PPMS instrument using a hybrid adiabatic relaxation method. The two-tau relaxation method was used to determine the heat capacity with the PPMS software.

Other Studies. Infrared spectra were recorded in the solid state (KBr pellets) on a Perkin-Elmer PARAGON 1000 FT-IR spectrometer in the $400\text{--}4000$ cm^{-1} range. Elemental analyses have been carried out by using a Perkin-Elmer TGA-7 TG analyzer.

1. Sheldrick, G. M. *SHELXL-97*; University of Gottingen: Gottingen, Germany, 1997.
2. Boudreaux, E. A.; Mulay, L. N. *Theory and Application of Molecular Paramagnetism*, Wiley J. & Sons, New York, 1976; p. 491.

Table 1S. Crystallographic data for complex **1**

1	
Empirical formula	C ₁₀ H ₈ CoN ₂ O ₄
Formula weight	279.11
Temperature	200(2) K
Wavelength	0.71073 Å
Crystal system	Monoclinic
Space group	<i>P</i> 2 ₁ / <i>c</i>
Unit cell dimensions	<i>a</i> = 10.840(3) Å <i>b</i> = 4.8670(14) Å <i>c</i> = 19.354(6) Å
Volume	1018.4(5) Å ³
<i>Z</i>	4
Density (calculated)	1.365 Mg/m ³
Absorption coefficient	1.266 mm ⁻¹
<i>F</i> (000)	423
Crystal size	0.4 x 0.1 x 0.3 mm ³
Theta range for data collection	1.88 to 28.58°
Index ranges	-14 ≤ <i>h</i> ≤ 14, -5 ≤ <i>k</i> ≤ 6, -17 ≤ <i>l</i> ≤ 26
Reflections collected	7171
Independent reflections	2579 [R(int) = 0.0343]
Completeness to theta = 25.00°	99.0%
Absorption correction	Semi-empirical from equivalents
Refinement method	Full-matrix least-squares on <i>F</i> ²
Data / restraints / parameters	2579 / 0 / 156
Goodness-of-fit on <i>F</i> ²	1.045
Final <i>R</i> indices [<i>I</i> > 2σ(<i>I</i>)]	<i>R</i> 1 ^a = 0.0354, <i>wR</i> 2 ^b = 0.0911
<i>R</i> indices (all data)	<i>R</i> 1 = 0.0444, <i>wR</i> 2 = 0.0962
Largest diff. peak and hole	0.743 and -0.711 e.Å ⁻³

$${}^a R1 = (\sum ||F_o| - |F_c||) / \sum |F_o| \quad {}^b wR2 = [\sum [w(F_o^2 - F_c^2)^2] / \sum [w(F_o^2)^2]]^{1/2}$$

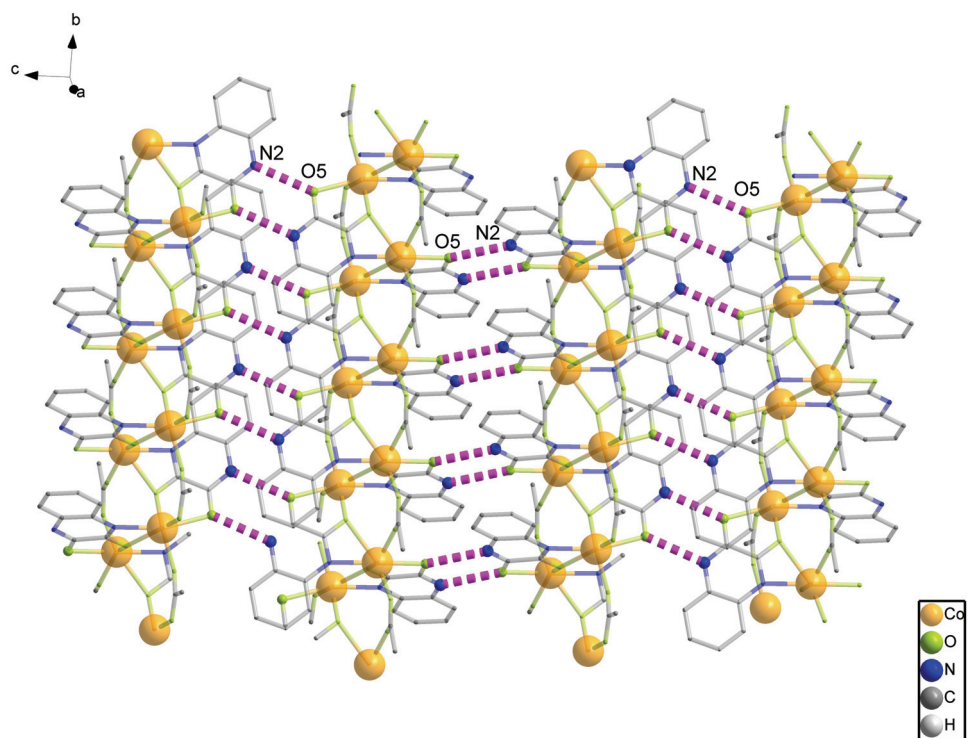


Figure 1S. 2D layer structure of **1** connected by H bonding.

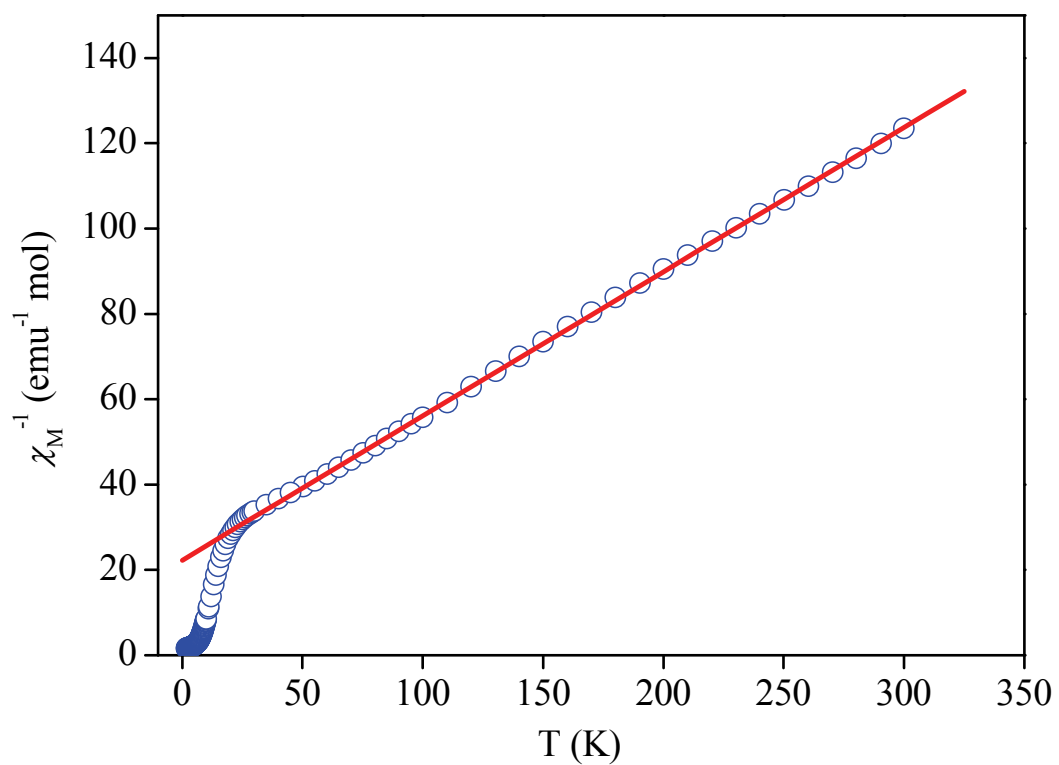


Figure 2S. Plot of χ_M^{-1} (○) vs. temperature for a microcrystalline sample of complex **1**. The solid line represents the best fit χ_M^{-1} above 50 K with a Curie–Weiss law.

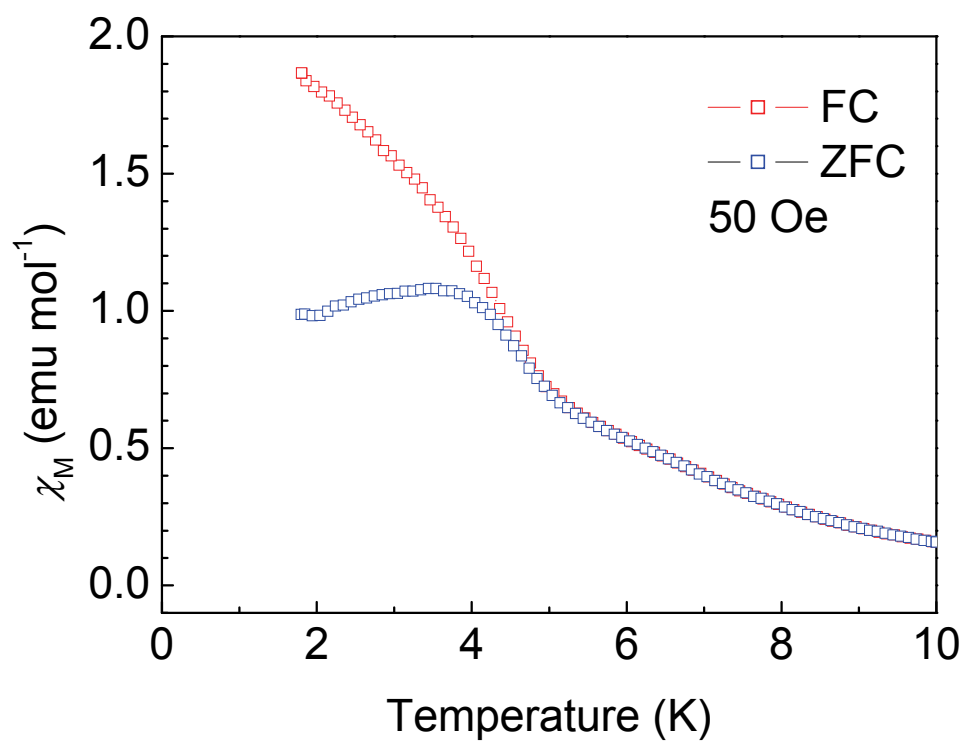


Figure 3S. ZFC/FC magnetization for **1** at an applied field of 50 G.

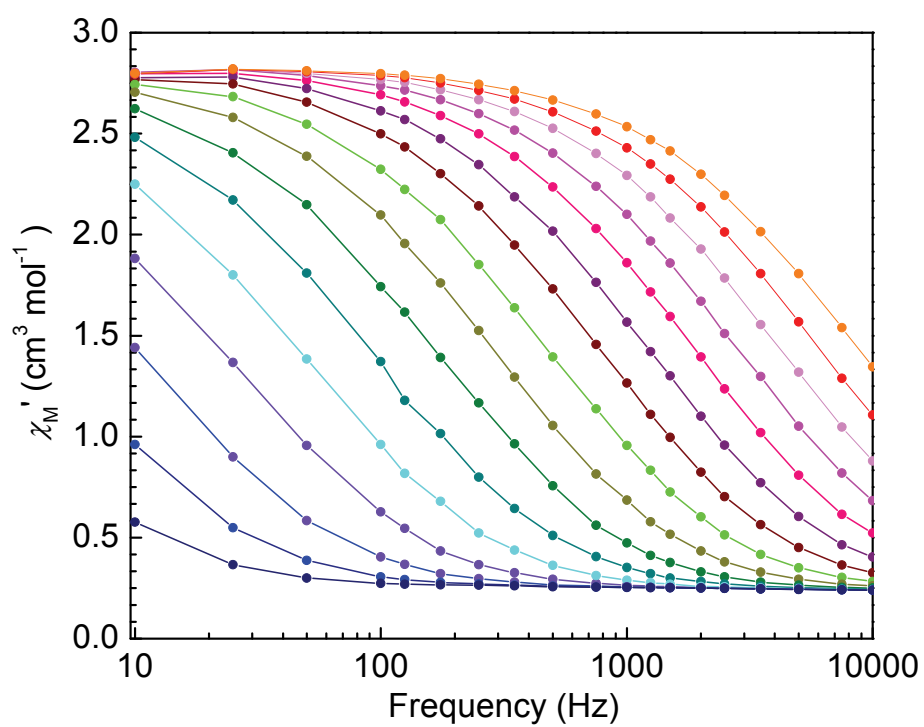


Figure 4S. Plots of in-phase (χ_M') of ac susceptibility vs. frequency in a 3.5 G ac field oscillating at the indicate temperatures for complex **1**.

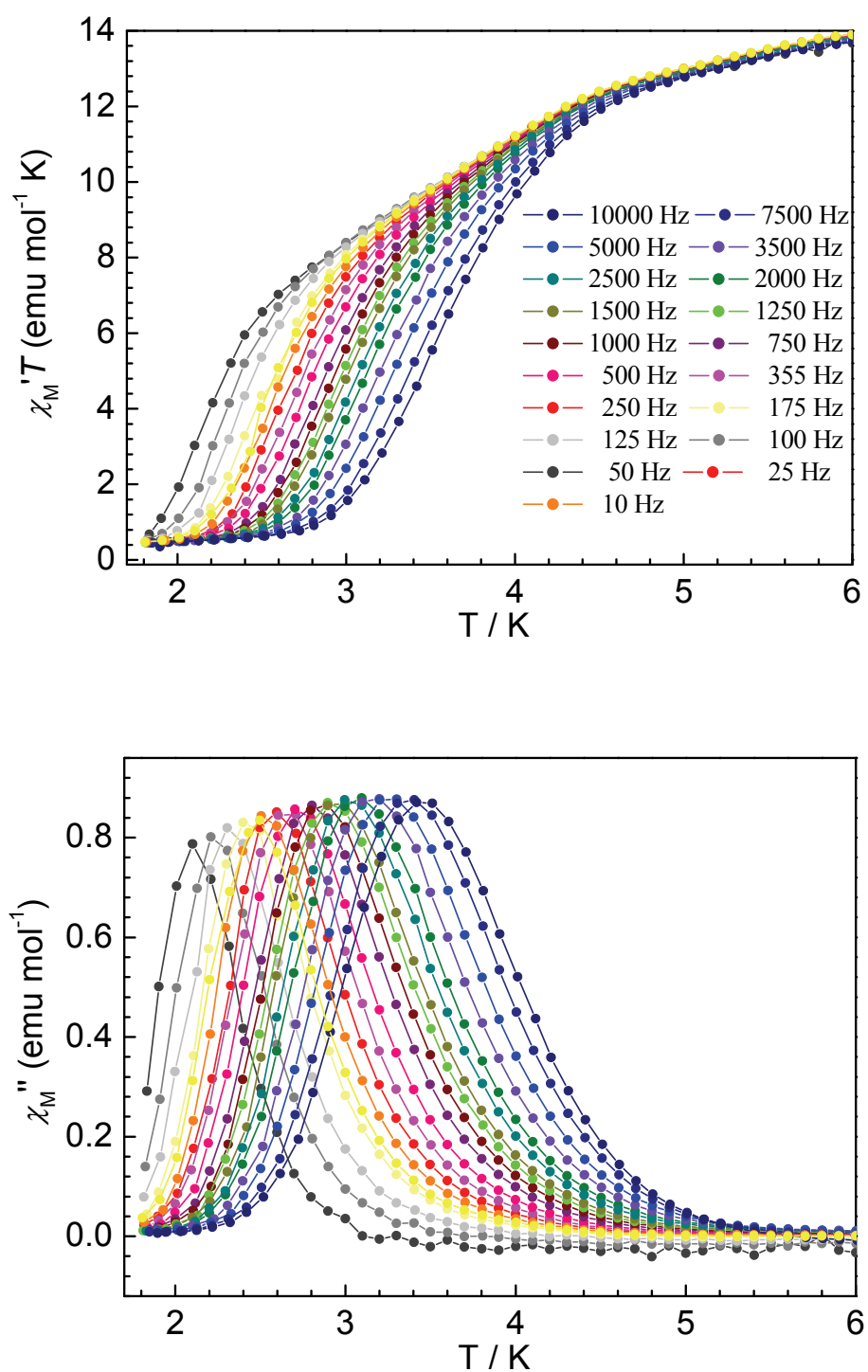


Figure 5S. Plots of in-phase ($\chi_M' T$) (Top) and out-of-phase (χ_M'') (Bottom) of ac susceptibility vs. T in a 3.5 G ac field oscillating at the indicate frequencies for complex **1**.

A scaling procedure of the $\chi_M T$ data for **1** (Figure 6S) clearly indicates a linear regime characteristic of Ising 1D systems. The $\ln(\chi_M' T)$ versus $1/T$ plot increases linearly between 8 and 14 K, with an energy gap, Δ_ξ , of 16 K. It should be noted that the ΔE barrier extracted from the ac data is significantly larger than Δ_ξ , suggesting that the relaxation mechanism in this SCM cannot be described by a simple Glauber model.³

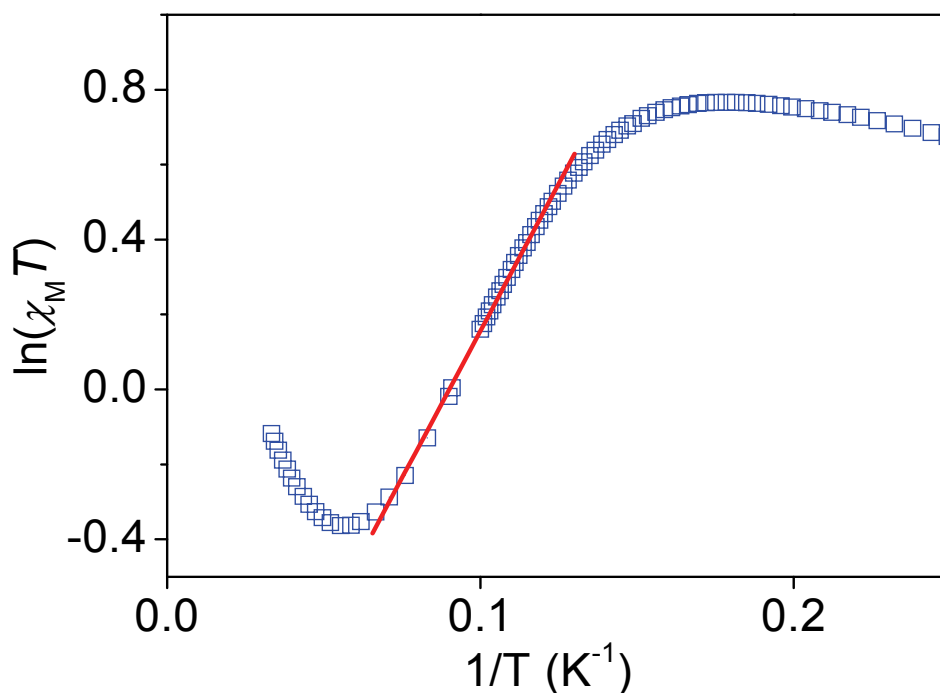


Figure 6S. Plot of $\ln(\chi_M' T)$ vs. T^{-1} for **1**. Solid line represents the fit of $\chi T = C_{\text{eff}} \exp(\Delta_\xi/k_B T)$ between 8 and 14 K.

3. C. Coulon, R. Clérac, L. Lecren, W. Wernsdorfer, H. Miyasaka, *Phys. Rev. B* 2004, **69**, 132408.

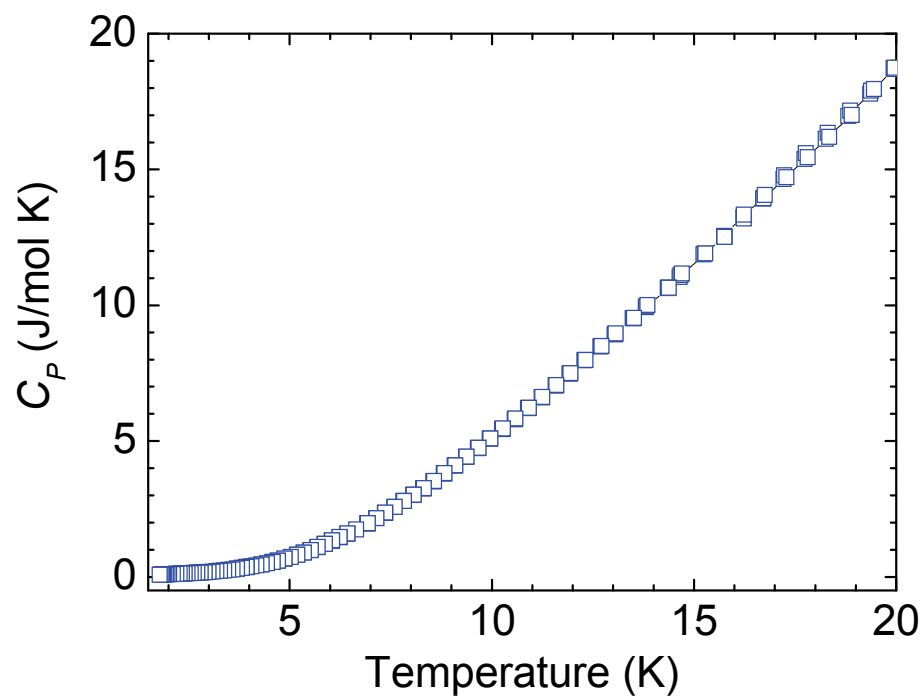


Figure 7S. Plot of C_p vs. T for a pellet piece polycrystalline of **1** measured on grounded crystals under zero applied field.